HEAT TRANSFER BY THE SIDE WALL OF AN ALUMINUM ELECTROLYSIS CELL

Marin V. PETRE[1], Alexandru M. MOREGA[2]

Acest articol prezinta o analiză a problemei transferului de căldură la peretele lateral al chesonului unei cuve de electroliza de la uzina ALRO Slatina. Întrucât odată cu creşterea intensităţii curentului electric creşte şi căldura internă produsă în celula de electroliză, trebuiesc identificate căi şi mijloace de disipare ale căldurii în exces. Una dintre soluţii constă în modificarea designului de cuvă actual, prin modificarea peretelui chesonului. Lucrarea prezintă rezultate de simulare şi experimentale referioare la cele două variante constructive de cheson – clasică şi modificată. Rezulatele obţinute pot fi utile în optimizarea proiectării cuvelor de electroliză.

This paper presents the heat transfer by the side-wall of an electrolysis cell in ALRO Slatina plant. Because internal heat generation increases with the electrical power density, adequate ways and means of dissipating the heat in excess must be considered. One of the solutions consists in redesigning the current cell wall. The paper presents simulation and experimental results that may be of interest in to the cell case design.

Keywords: aluminum electrolysis, heat transfer modeling, finite element

1. Introduction

Aluminum production by electrolysis is one of the most energy-intensive processes therefore improving its efficiency is a matter of concern. Modern electrolysis cells are rated at very high currents, *e.g.*, 500 kA [1]-[5]. Since by increasing the electrical current the generation of internal heat increases too, ways and means to dissipate the heat surged in excess are needed. One of the solutions consists of modifying the pot design, and this approach is used at ALRO plant in Slatina. A new cell design was produced, and experiments carried on. A group of 15 cells was selected, and specialized equipment for measuring the temperature out of the cell's shell were utilized (*e.g.*, thermocouples, Fluke thermo-camera [6]). To evaluate the cell design, periodically, some of the cells in the testing group were examined. On the other hand, an electro-thermal mathematical model of the cell was formulated, and solved numerically by the finite element technique

[1] ALRO Slatina Plant, Slatina, Romania
[2] Prof., Faculty of Electrical Engineering, University POLITEHNICA of Bucharest, Romania, amm@iem.pub.ro

[4]. This paper reports simulation results that were obtained. Experimental data was input to the model aiming at providing accurate working conditions, and thus better depicting the heat transfer mechanisms from the cell shell to the ambient.

2. The Side-Wall Model

The initial design of the cell's metallic shell is sketched in Fig.1,*a* [2]: the shell is braced by a bridge (*a*), and consolidated with an *L*-shaped belt (*b*) coming from beneath. At the metal bath interface level, a horizontal *I*-shaped belt clasps the shell (*c*). A second, *I*-shaped belt, with the same characteristics as the first one, strengthens the shell at the sub-cathode level (*d*). Several pillars, placed between the walls of two adjacent cells, restrict the shells side-walls bending. These three structural elements – the belts, the *I*-shaped bridges, and the pillars – in the original design were not sturdy enough and, consequently, the side-wall bowed by 10-30 mm through thermal deformation.

The bending of the cell is acceptable for the cells with side feeding where the side-wall deformation is a consequence of feeding and of the crust plunging. The deformation is still acceptable at the cells with central feeding with large side channels (*i.e.*, the distance between the anode and the side slab) of 45 to 60 mm, working at relatively low-density anodic currents [2].

However, the risk of perforation increases significantly for 120 kA cells where the side channel is shrunk and the bending is relatively high. Consequently, a major redesign of the 120 kA cells shell was needed. The new design (Fig.1) had to account for the increase of shell wall temperature by 24 °C.

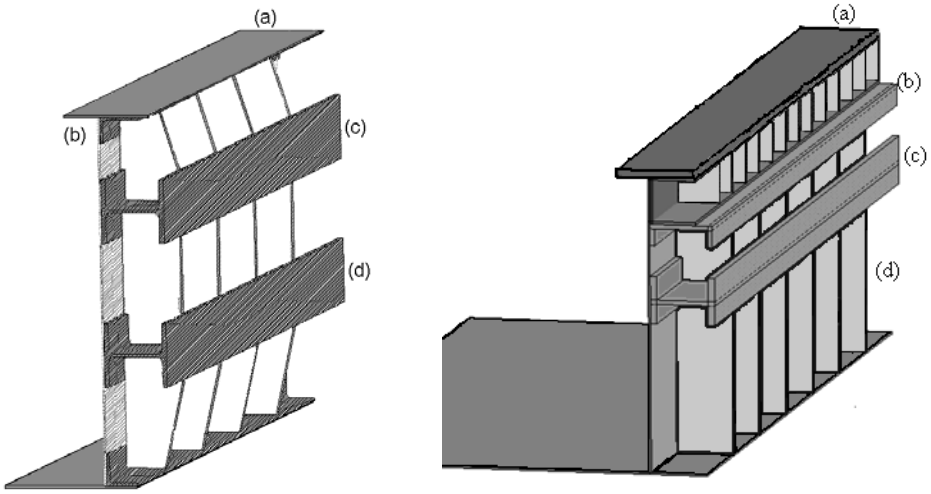

a. Shell used until 2002 [2]. ***b.*** New design [2].

Fig.1. Shells for the 120 kA cell – old and new designs, partial views.

The new shell proposed for 120 kA is provided with new structural elements (Fig.1,*b*): an upper, removable plate (*a*); two belts on the side-wall (*U*-shaped (*b*), and *I*-shaped (*c*), respectively) interconnected by vertical belts (*d*).

In this study we are concerned with investigating the heat transfer through the side-walls of the shell and in the spacing between two adjacent shells. Next, we present the mathematical model and numerical simulation results for the heat transfer from the cell shell side-wall to the ambient.

3. The Mathematical Model

Figure 2 shows a qualitative sketch of the 2D cross-sectional view of interval between two adjacent shells investigated in the heat transfer model.

a. Half space between two adjacent shells. ***b.*** FEM mesh (10896 triangular elements)

Fig.2. The computational domain: The right margin is a symmetry plane.

The mathematical model that we developed accounts for the heat transfer by natural convection in the spacing between two adjacent cells. We assume the (air) flow is incompressible, laminar, and neglect the radiation heat transfer between the shells and surrounding space (7), (8).

A. The flow part of the problem, is made of the following equations

momentum balance (*Navier-Stokes*)

$$\rho(\mathbf{u}\cdot\nabla)\mathbf{u} = \nabla\cdot\left[-p\mathbf{I} + \eta\left(\nabla\cdot\mathbf{u} + (\nabla\cdot\mathbf{u})^{T}\right)\right] + \mathbf{f}\,, \tag{1}$$

mass conservation

$$\nabla \cdot \mathbf{u} = 0. \tag{2}$$

Here ρ is the mass density, η is the dynamic viscosity, **f** is the gravitational body force (buoyancy), *p* is the pressure, **I** is the unit matrix and **u** is the velocity.

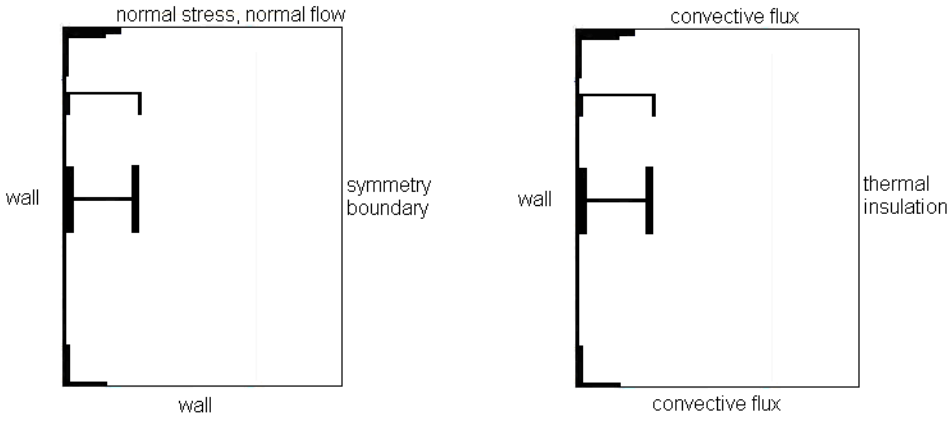

a) Thermal flow. b) Heat transfer.

Fig.3. The boundary conditions for natural convection heat and flow.

The boundary conditions for the flow part of the problem are as follows (Fig.3,*a*):

the walls (steel structure)

$$\mathbf{u} = 0, \tag{3}$$

the horizontal, upper free surface

$$\mathbf{n} \cdot \left[-p\mathbf{I} + \eta\left(\nabla \cdot \mathbf{u} + (\nabla \cdot \mathbf{u})^T\right)\right] = f_0 \mathbf{n}, \quad \mathbf{t} \cdot \mathbf{u} = 0, \tag{4}$$

the vertical, symmetry boundary

$$\mathbf{t} \cdot \left[-p\mathbf{I} + \eta\left(\nabla \cdot \mathbf{u} + (\nabla \cdot \mathbf{u})^T\right)\right] = 0, \quad \mathbf{n} \cdot \mathbf{u} = 0. \tag{5}$$

B. The heat transfer part of the problem is made of the energy equation (6)

$$\nabla \cdot (-k\nabla T) = -\rho C_p \mathbf{u} \cdot \nabla T. \tag{6}$$

The following boundary conditions (Fig.3, *b*) close the heat transfer model

on the bottom surface

$$-\mathbf{n}\cdot(k\nabla T)=0, \tag{7}$$

on the (top) open surface and the symmetry (*right*) *plane*

$$\mathbf{q}=-k\nabla T+\rho C_p T\mathbf{u}, \tag{8}$$

on the shell wall (Fig.3,*b*)

$$T_w=T(x=0,y). \tag{9}$$

Here T is the temperature, k is the thermal conductivity of air, C_p is the specific heat of air at constant pressure, ρ is the density of air, and **u** is the velocity field.

Thermal vision camera [6] measurements were used to assess the thermal load of the shell. In particular, temperature measurements by the side-walls of the shell indicate a higher temperature area in the area of the two side belts of the shell, which, in fact are the areas that bear the highest risk of perforation.

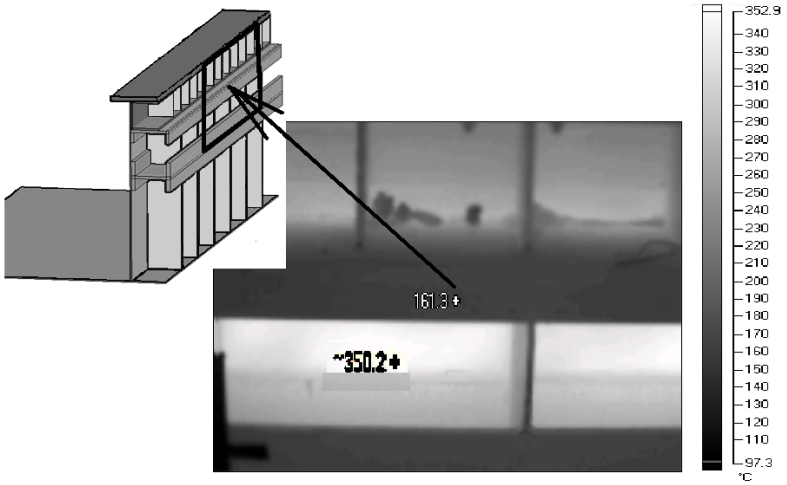

Fig.4. Thermo-vision image of the spacing between the shell side belts.

We utilized thermo-vision images to find the shell wall temperature. It is very important to choose a proper value for emissivity in order to obtain accurate temperature readings with the thermal vision camera. To comply with, we used three types of equipments to perform this measurement. We used the thermal vision camera [6], normal contact thermocouples, and a laser measuring

equipment. By utilizing these we obtained for emissivity the value 0.94.

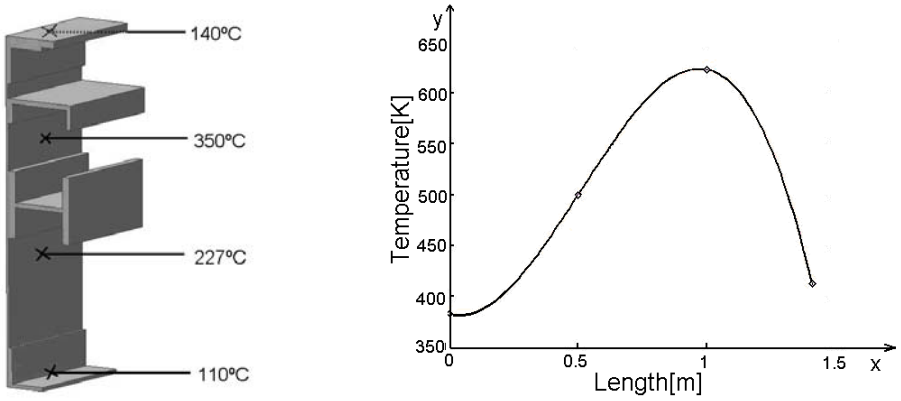

a) Temperature on the wall – empiric data. b) Interpolated thermo-vision data.

Fig.5. The wall temperature was obtained by interpolating thermo-vision data, used next as boundary condition.

Figure 5 shows the temperature profile produced by this technique when utilizing a third order interpolating polynomial that is input as boundary condition. A Matlab [13] program is used to implement this algorithm.

4. Results and Discussion

The mathematical model (1)-(9) was solved numerically by the Galerkin finite element method (FEM) as implemented by Comsol Multiphysics [10]. Material properties were obtained from the available literature – *e.g.*, [10], [11].

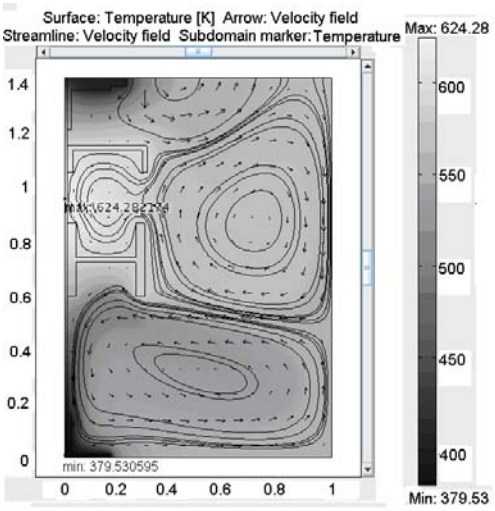

Fig.6. Heat transfer by the cell side wall. Excessive temperature is registered in the region confined between the horizontal belts.

Figure 2,*b* shows the FEM unstructured discretization mesh made of triangular elements. The simulation results unveil insights of the natural convection flow and paths. For instance, Fig. 6 reports the temperature in the space between shells. A high temperature area located between the two horizontal belts is noticeable. The shell wall experiences a high temperature variation, suggesting that thermally induced mechanic stress may occur, a menace to the shell life.

The natural convection flow field obtained by simulation (Fig. 7) explains this situation: the two belts act as a cavity that traps air, as evidenced by the recirculation cell that develops in this region. Heat transfer from this cell to the free space between two adjacent shells occurs mainly through diffusion (almost no convection). The heat transfer transferred from the cell to the ambient is thus reduced, and the consequence is the excessive temperature of this region. It is suggested that shell perforation may more probably occur somewhere in this area.

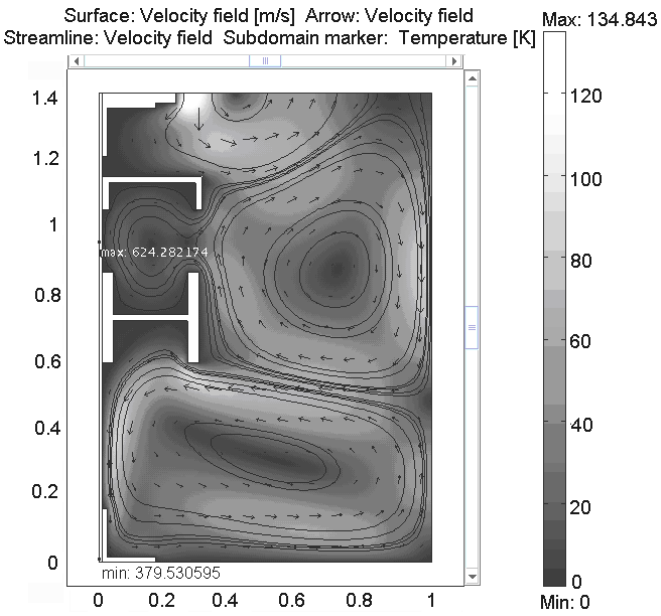

Fig.7. The natural convection flow field.

In this study, as stated, it was assumed that the space between two neighbor cells possesses symmetry with respect to a vertical plane, which subsequently suggests that a reduced, “half-space” may be acceptable. To check the accuracy of this assumption we consider the simplified model and also the

model of the entire inter-cells spacing (the "whole space" model).

The simulation results show similar spectra for the velocity field and for the temperature. The heat flux (Fig.8,*b*) and temperature (Fig.9) along the symmetry plane in the two models (the line marked in Fig.8,*a*) are similar within acceptable numerical accuracy limits – the two curves actually overlap.

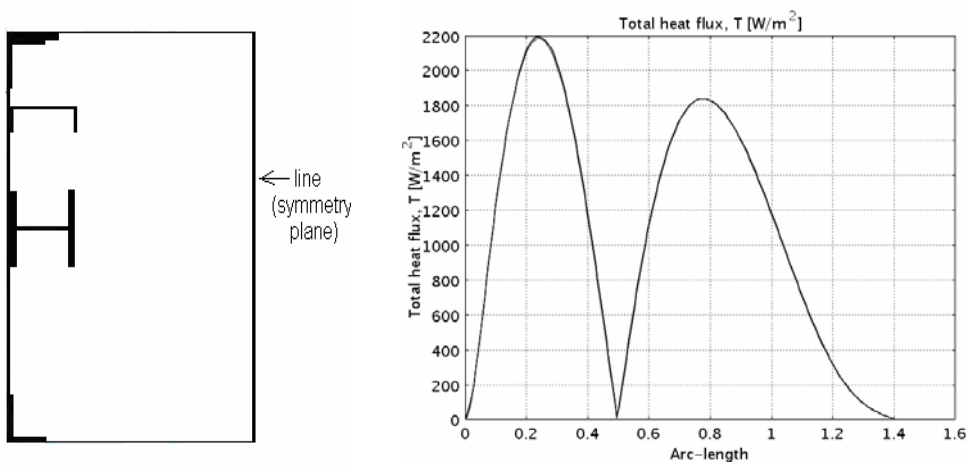

a) Half space between two adjacent shells and the symmetry plane.

b) The total heat flux along the symmetry plane in the two models.

Fig.8. The total heat flux [W/m²] along the symmetry plane.

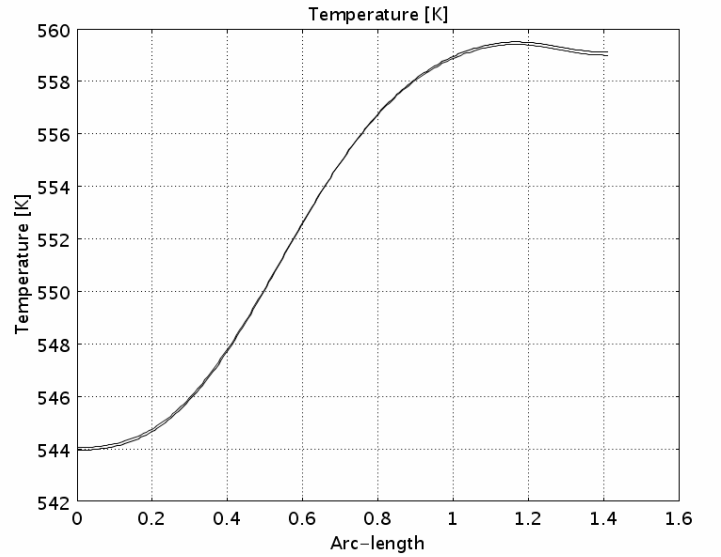

Fig.9. The temperature along the symmetry plane in the two models.

Another important result is that the total heat flux (Fig.10) conveyed throughout the spacing between the horizontal belts is small. Therefore particular attention should be devoted to assess the consequences that this effect may have on the thermal stability of the cell in this area.

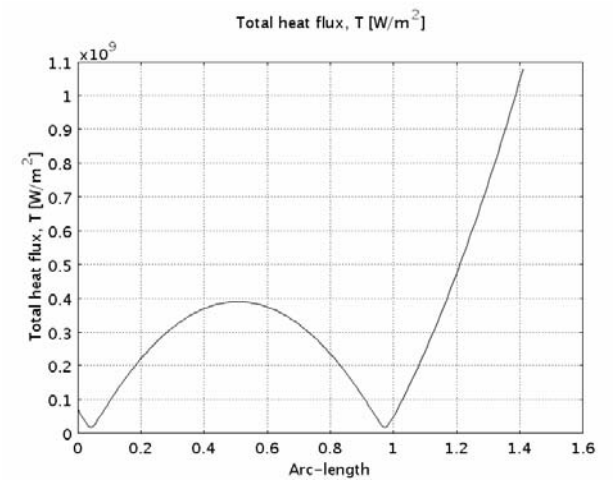

Fig.10. The total heat flux for the left side of the shell cell.

It was recorded and documented that experimental observations show-off that at this level (corresponding to the hot-spot region) the molten aluminum layer is approximately located. It is also known that this region is more likely prone to perforation – a fault condition for the electrolysis cell. On the other hand, the heat flux transferred from the wall to the ambient by the other parts of the cell wall is considerable larger.

5. Conclusions

The numerical study presented in this paper, based on experimental results (*e.g.*, the wall temperature is extracted from thermo-vision images) provides valuable information concerning the heat transfer from the shell to the surroundings.

Experimental data was used to specify the temperature distribution on the case wall. The shell wall design may be improved, *e.g.*, by repositioning and reshaping the structural elements (belts), to reduce the thermal load and stresses experienced by walls.

To assess the validity of the half-space model (defined by invoking symmetry) we considered also the model of the entire spacing between cells (the so-called “whole space” model). We verified that the heat flux and temperature

profiles along the symmetry plane (line in the 2D analysis) in the two models are almost identical.

The simulations results are in good agreement with experimental (temperature) data obtained by means of thermo-vision camera – this is an important part for the experimental validation.

Future work will address a more realistic, 3D model for the shell, and the optimization of the shell wall design to enhance the airflow in the area between the two belts.

ACKNOWLEDGMENTS

The work was conducted in the Laboratory for Multiphysics Models at the Faculty of Electrical Engineering, PUB. The authors gratefully acknowledge ALRO-Slatina plant support in carrying out the experimental work embodied herein. Eng. Cr. Stănescu's comments and advises are highly appreciated.

R E F E R E N C E S

[1] *M. Repetto*, *I. Panaitescu*, *K. Pericleous*, *L. Leboucher*, *V. Chechurin*, *A. Kalimov*, *A. Moraru*, *A. Panaitescu*, *A.M. Morega*, *D. Mocanu*, Optimisation of an electrolysis cell for aluminum production, OPTIM 2000, Braşov, 11-12 May, 2000.

[2] *Cr. Stanescu*, *Gh. Dobra*, *Gh. Rădulescu*, *C. Rădulescu*, Increasing the aluminum electrolysis cell productivity, S.C. ALRO S.A., 2008, S.R.M.

[3] *C. Vanvoren, P. Homsi, JL. Basquin, T. Beheregaray,* AP 50: The Pechiney 500 kA Cell, Light Metals, 2001, pp 221-227.

[4] *A.M. Morega*, *V.M. Petre*, *A. Panaitescu*, Current flow and heat transfer in aluminum electrolysis cell – a FEM Analysis, *ATEE 2006*, Bucharest, 2006.

[5] *D. Mocanu*, *A.M. Morega*, *A. Panaitescu*, *I. Panaitescu*, *A. Moraru*, Current flow and heat transfer processes in Aluminum electrolysis cells, *8th IGTE Symposium*, Technical University of Graz, Austria, 1998.

[6] Smartview 1.8.0.6, 2006, Fluke Thermography, 3550 Annapolis Lane, Plymouth, MN 55447, USA.

[7] *N. Munteanu*, *D.D. Popescu*, *M. Cilianu*, *M. Modan*, *P. Stanciu*, The measurement of the temperature on the exterior surface of the cell depending on the reference voltage and the medium height of the molten metal between two extractions, WP 3.2, ALELINCO/Copernicus IC 15-CT 96-0714, IMNR Bucharest, 1997.

[8] *A. Bejan*, Heat Transfer, J. Wiley, NY, 1992.

[9] *A.M. Morega*, Principles of Heat Transfer, in Handbook of Mechanical Engineering, Academic Press, 2001.

[10] COMSOL, v. 3.4, Comsol AB, Sweden, 2008.

[11] Materials Properties Database, MPDB v. 3.02, JAHM Software Inc., USA, 2000.

[12] Autodesk Inventor 2009, Autodesk, San Rafael, California, USA.

[13] MathWorks, MATLAB, v. R2008b.